J. Astrophys. Astr. (2019) 40:41
https://doi.org/10.1007/s12036-019-9610-5

Review

Cold neutral hydrogen gas in galaxies

RAJESHWARI DUTTA

European Southern Observatory, Karl-Schwarzschild-Str. 2, 85748 Garching Near Munich, Germany.
E-mail: rdutta@eso.org

MS received 29 June 2019; accepted 18 September 2019

Abstract. This review summarizes recent studies of the cold neutral hydrogen gas associated with galaxies probed via the HI 21-cm absorption line. HI 21-cm absorption against background radio-loud quasars is a powerful tool to study the neutral gas distribution and kinematics in foreground galaxies from kilo-parsec to parsec scales. At low redshifts ($z < 0.4$), it has been used to characterize the distribution of high column density neutral gas around galaxies and study the connection of this gas with the galaxy's optical properties. The neutral gas around galaxies has been found to be patchy in distribution, with variations in optical depth observed at both kilo-parsec and parsec scales. At high redshifts ($z > 0.5$), HI 21-cm absorption has been used to study the neutral gas in metal or Lyman $-\alpha$ absorption-selected galaxies. It has been found to be closely linked with the metal and dust content of the gas. Trends of various properties like incidence, spin temperature and velocity width of HI 21-cm absorption with redshift have been studied, which imply evolution of cold gas properties in galaxies with cosmic time. Upcoming large blind surveys of HI 21-cm absorption with next generation radio telescopes are expected to determine accurately the redshift evolution of the number density of HI 21-cm absorbers per unit redshift and hence understand what drives the global star formation rate density evolution.

Keywords. Galaxies—absorption lines—interstellar medium.

1. Introduction

The interstellar medium (ISM) of a galaxy is a complex and dynamic system with constant interplay of matter, momentum and energy between the various ISM phases and the stars. The phase structure of the ISM is hence a direct probe of various complex astrophysical processes that take place inside a galaxy. In addition, the ISM mediates between the stellar- and the galactic-scale processes. The accreting ionized gas from the intergalactic medium (IGM) passes though the different ISM phases before getting converted to stars. On the other hand, galactic winds, outflows and fountains populate the IGM with metals. Diffuse ionized hydrogen gas and metals have been observed to extend up to few hundreds of kilo-parsec around galaxies, constituting the circumgalactic medium (CGM; Tumlinson *et al.* 2017). The large-scale multi-phase gas distribution in the CGM around galaxies, due to infalls, outflows and mergers, is again intricately linked with the ISM and the star formation in galaxies. Therefore, the ISM and CGM phases are expected to contain an imprint of the collective outcome of all the processes that shape the star formation history of the Universe (Hopkins & Beacom 2006).

In this review, we focus on the neutral gas phase in and around galaxies. In particular, we review studies of the cold neutral hydrogen gas as probed using the tool of HI 21-cm absorption. In Sections 2 and 3, we introduce the neutral gas phase and HI 21-cm absorption, respectively. We discuss results from studies of distribution of cold neutral gas around low-z galaxies in Section 4, dependence of cold neutral gas on metals and dust at high-z in Section 5, and the redshift evolution of cold gas properties in Section 6. We conclude by discussing future prospects in Section 7.

2. The neutral gas phase

The neutral gas phase in and around galaxies acts as the intermediary phase between the accreting ionized gas from the IGM and the molecular gas phase in the stellar disc that gets converted to stars. It thus is the reservoir from which molecules and stars form and

Published online: 10 October 2019

consequently plays a crucial role in galaxy formation and evolution. The HI disc around galaxies is the component that gets affected the most by tidal interactions and mergers, since it is more extended than the stellar disc, typically by more than a factor of two (Haynes *et al.* 1979; Rosenberg & Schneider 2002; Oosterloo *et al.* 2007; Sancisi *et al.* 2008; Chung *et al.* 2009; Mihos *et al.* 2012). Therefore, in the hierarchical structure formation models, galaxy formation is expected to leave its imprint on the atomic gas mass density and its evolution with redshift.

The neutral gas exists in two dominant phases, the cold neutral medium (CNM; $T \sim 100\,\mathrm{K}, n \sim 30\,\mathrm{cm}^{-3}$) and the warm neutral medium (WNM; $T \sim 10^4\,\mathrm{K}$, $n \sim 0.3\,\mathrm{cm}^{-3}$). Field *et al.* (1969) demonstrated that the CNM and the WNM can coexist in pressure equilibrium, such that the neutral gas can be considered as a two-phase medium. Observations of the Milky Way and nearby galaxies also provide evidence for a two-phase neutral medium (e.g. Dickey *et al.* 1983; Kulkarni & Heiles 1987; Wolfire *et al.* 1995; Mebold *et al.* 1997; Braun 1997; Dickey *et al.* 2000). Wolfire *et al.* (1995) and Wolfire *et al.* (2003) investigated the thermal balance of the WNM and CNM phases in the Galactic ISM. They found that their two-phase model, with thermal pressure in the range $\sim 10^{3-4}\,\mathrm{K\,cm}^{-3}$, is in good agreement with observations of the Galactic ISM. In addition, the pressure equilibrium in their model depends on the gas phase abundance, dust abundance, metallicity, absorbing column density and radiation field. However, note that Heiles & Troland (2003) found that a large fraction, i.e. about 50% of the WNM lies in the thermally unstable region of 500–5000 K. The heating mechanisms in the neutral ISM are dust photoelectric heating, cosmic ray heating, X-ray heating and heating by C I ionization, with dust photoelectric heating being the dominant heating mechanism. Radiative cooling by emission of the fine-structure lines, C II* $\lambda 158\mu$m and O I* $\lambda 63\mu$m, dominates at $n \gtrsim 1\ \mathrm{cm}^{-3}$ ($T \lesssim 2000\,\mathrm{K}$), while electron recombination onto positively charged grains and radiative losses from resonant transitions like Lyman-α dominate at $n \lesssim 0.1\ \mathrm{cm}^{-3}$ ($T \gtrsim 7000\,\mathrm{K}$).

3. HI 21-cm absorption

The neutral gas in the ISM can be detected and studied via the HI 21-cm line, which originates in the hyperfine splitting of the 1*s* electronic ground state of hydrogen atom. Predicted by H.C. Van de Hulst in 1945 (van de Hulst 1945), HI 21-cm emission from our Galaxy was first detected in 1951 (Ewen & Purcell 1951; Muller & Oort 1951; Pawsey 1951). Since then the HI 21-cm emission line has proved to be a powerful tool for studying the distribution, amount, kinematics, and temperature of the neutral gas in our Galaxy as well as other galaxies. In the local Universe ($z \lesssim 0.2$), blind HI 21-cm emission-line surveys using single-dish telescopes have provided reliable measurements of the cosmological HI mass density (Rosenberg & Schneider 2002; Zwaan *et al.* 2005a; Hoppmann *et al.* 2015; Jones *et al.* 2018), and spatially resolved HI imaging using interferometers have traced the large scale dynamics of galaxies (van der Hulst *et al.* 2001; Zwaan *et al.* 2001; Verheijen *et al.* 2007; de Blok *et al.* 2008; Walter *et al.* 2008; Begum *et al.* 2008; Catinella & Cortese 2015). Rotation curves derived from HI 21-cm emission maps of galaxies have provided evidence for the existence of dark matter (Bosma 1978, 1981a, b; van Albada *et al.* 1985; Rubin *et al.* 1985; Begeman 1987; Broeils 1992). However, the flux of the HI 21-cm emission signal is inversely proportional to the square of the distance to the unresolved emitting gas. Hence, sensitivities of present day radio telescopes make it difficult to directly map HI emission from $z \gtrsim 0.2$ galaxies. The highest redshift ($z = 0.376$) HI 21-cm emission detection to date (Fernández *et al.* 2016) has been possible due to very long integration (178 hours) using the Karl G. Jansky Very Large Array (VLA). Besides direct detection of HI 21-cm emission from galaxies, there have been several HI 21-cm emission line stacking experiments which have studied the average HI properties of different samples of galaxies (Lah *et al.* 2007, 2009; Delhaize *et al.* 2013; Rhee *et al.* 2013, 2018; Kanekar *et al.* 2016). In addition to stacking, intensity mapping and cross-correlation of HI 21-cm emission with optical galaxy surveys (e.g. Chang *et al.* 2010; Masui *et al.* 2013) can complement individual HI line surveys and probe the average HI emission of galaxies upto higher redshifts ($z \sim 1$).

Unlike HI 21-cm emission, the detectability of HI 21-cm absorption is not limited by distance of the absorbing gas and depends only on the strength of the background radio sources and HI 21-cm absorption cross-section projected on the sky by the galaxies. Therefore, HI 21-cm absorption line studies can complement the emission line surveys to trace the evolution of the atomic gas component in galaxies. The first Galactic detections of HI 21-cm absorption were reported by Hagen *et al.* (1954), Hagen & McClain (1954) and Hagen *et al.* (1955). Clark *et al.* (1962) was the first to use extragalactic radio sources to probe Galactic HI 21-cm absorption, followed by Shuter & Gower (1969) and Heiles & Miley (1970). The first detection of extragalactic HI 21-cm absorption was from the radio galaxy, Centaurus A

(Roberts 1970). Thereafter, Brown & Roberts (1973) detected HI 21-cm absorption at $z = 0.692$ towards the background quasar 3C 286. Subsequently, HI 21-cm absorption has been used to probe the atomic gas in galaxies upto higher redshifts (see Kanekar *et al.* 2014, for a compilation), starting with detections of HI 21-cm absorption at $z > 1$ by Wolfe & Davis (1979), Wolfe *et al.* (1981) and Wolfe *et al.* (1985).

Further, HI 21-cm emission line observations of nearby dwarf and spiral galaxies indicate that properties of the CNM phase and ∼100 pc- to 2 kpc-scale structures detected in the HI gas are closely linked with the in-situ star formation in galaxies (e.g. Tamburro *et al.* 2009; Bagetakos *et al.* 2011; Ianjamasimanana *et al.* 2012). However, identification of CNM gas through HI 21-cm emission is not straightforward as it depends on Gaussian decomposition of the emission line profiles. In the absence of absorption line measurements, it is not known whether the HI 21-cm emission line components exhibiting smaller line widths (and hence assumed to correspond to CNM) are truly cold. Therefore, the contributions due to turbulent motions and the processes driving the observed properties of HI gas are poorly constrained. Moreover, HI 21-cm emission studies usually do not have sufficient spatial resolution to detect parsec-scale structures. On the other hand, HI 21-cm absorption is an excellent tracer of the CNM phase (Kulkarni & Heiles 1988), and can be used to study parsec-scale structures in the HI gas using sub-arcsecond-scale spectroscopy (e.g. Srianand *et al.* 2013).

The HI 21-cm optical depth integrated over velocity ($\int \tau \mathrm{dv}$ in $\mathrm{km\,s^{-1}}$) is related to the column density of neutral hydrogen, $N(\mathrm{HI})$ ($\mathrm{cm^{-2}}$), spin temperature T_s (K) of the gas, and the fraction C_f of the background radio source covered by the absorbing gas, as (e.g. Rohlfs & Wilson 2000):

$$N(\mathrm{HI}) = 1.823 \times 10^{18} \frac{T_\mathrm{s}}{C_\mathrm{f}} \int \tau \mathrm{dv}, \qquad (1)$$

where the HI 21-cm line is assumed to be optically thin. Note that if there are a number of HI gas clouds at different phases along the line-of-sight giving rise to the absorption line, then the effective T_s measured would be the column density-weighted harmonic mean of the T_s of the different clouds. The inverse dependence of the HI 21-cm optical depth on T_s, coupled with its very low transition probability and its resonance frequency falling in the radio wavelengths, make the HI 21-cm absorption line a good tracer of high column density cold HI gas without being affected by dust and luminosity biases. Hence, the HI 21-cm absorption line can be used to investigate:

1. the thermal state of the HI gas, since the HI 21-cm optical depth depends inversely on T_s, which is known to follow the gas kinetic temperature in the CNM (Field 1959; Bahcall & Ekers 1969; McKee & Ostriker 1977; Wolfire *et al.* 1995; Roy *et al.* 2006), and can be coupled to the gas kinetic temperature via the Lyman $-\alpha$ radiation field in the WNM in case of a two-phase medium (Liszt 2001);
2. the kinetic temperature of the gas can also be constrained using the thermal widths of the individual HI 21-cm absorption components, subject to the Gaussian modeling (e.g. Lane 2000; Kanekar *et al.* 2001);
3. the parsec-scale structure in the absorbing gas via sub-arcsecond-scale spectroscopy (e.g. Srianand *et al.* 2013; Biggs *et al.* 2016; Gupta *et al.* 2018b);
4. the magnetic field in the CNM using Zeeman splitting (Heiles & Troland 2004);
5. the filling factor of cold gas in the ISM/CGM of galaxies;
6. the underlying potential using the overall velocity width of the HI 21-cm absorption lines;
7. the temporal and spatial variation in fundamental constants of physics like electromagnetic fine structure constant, the proton-to-electron mass ratio and the proton g-factor (Wolfe *et al.* 1976; Carilli *et al.* 2000; Chengalur & Kanekar 2003; Kanekar *et al.* 2010, 2012; Rahmani *et al.* 2012).

Next, we discuss some of the limitations of the HI 21-cm absorption line technique. The main limitation when estimating $N(\mathrm{HI})$ from HI 21-cm absorption is that the two parameters – T_s and C_f in Equation 1, cannot usually be well-constrained. Comparison of both HI 21-cm emission and absorption spectra can be used to estimate T_s. Such studies are possible in our Galaxy and nearby galaxies (e.g. Wakker *et al.* 2011; Keeney *et al.* 2011; Dutta *et al.* 2016). Though it should be noted that the angular scales probed by HI 21-cm emission are usually larger than that by HI 21-cm absorption. Therefore, $N(\mathrm{HI})$ obtained from HI emission maps represents average HI surface density, while the cold gas traced by HI 21-cm absorption could be much clumpier, implying that there will be uncertainties in comparing HI emission to absorption. However, such comparisons of HI emission and absorption are not feasible at high redshifts as explained above. Hence, for identifying and studying the ISM of high redshift galaxies, one usually has to rely on absorption lines detected towards bright background sources like quasars and gamma ray bursts. In such cases, T_s can be estimated if there is

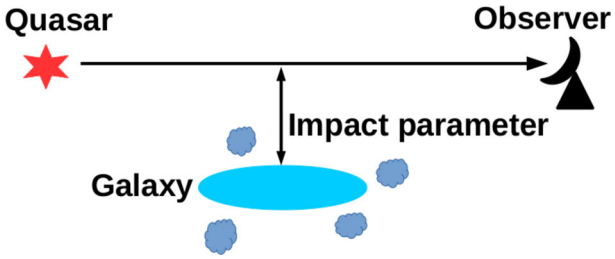

Figure 1. Schematic diagram to illustrate how spectra of background quasars are used to probe the gas around foreground galaxies. The projected separation between the quasar and galaxy is termed as the impact parameter.

independent measurement of N(HI) from Lyman $-\alpha$ absorption in optical or ultraviolet (UV) spectra. However, this technique suffers from uncertainties regarding how much of the HI gas traced by Lyman $-\alpha$ absorption is associated with the 21-cm absorbing gas, and whether the radio and optical lines-of-sight are aligned. The second parameter, C_f, is usually taken to be unity for lack of sufficient information about the extent of the absorber and the background radio source. This can be estimated by comparing the flux density of the radio source at high spatial resolution (parsec-scales), from Very Long Baseline Interferometry (VLBI) observations at the redshifted HI 21-cm line frequency, with the total flux density at the lower spatial resolution (usually kilo-parsec-scales) at which absorption is observed (e.g. Kanekar *et al.* 2009a; Gupta *et al.* 2012). However, VLBI observations of the radio sources may not always be available, especially at lower frequencies as required for the high redshift absorbers.

HI 21-cm absorption can be classified into two categories: (a) intrinsic and (b) intervening. The former probes neutral gas associated with the Active Galactic Nucleus (AGN) and its environment, and can be used to constrain models of formation and evolution of AGN, as well as the feedback they provide to their host galaxies (see for a review Morganti & Oosterloo 2018). The latter probes the neutral gas in foreground galaxies and can be used to study how galaxies form and evolve with time. Here we concentrate on the latter category. See Figure 1 for an illustration of quasar absorption line technique to study the gas associated with intervening galaxies.

4. Distribution of cold neutral gas around low-z galaxies

Absorption lines seen in the spectra of background quasars whose sightline happen to pass through the discs or halos of foreground galaxies (we refer to such fortuitous associations as quasar-galaxy-pairs or QGPs from hereon), allow us to probe the physical, chemical and ionization state of gas in different environments such as the stellar discs, extended HI discs, high velocity clouds, outflows, accreting streams and tidal structures. The main drawback of quasar absorption line spectroscopy is that it probes the gas only along the pencil beam sightline. This issue can be addressed by compiling a large homogeneous and statistically significant sample of absorbers. The relationship between absorption strength and impact parameter (projected separation between quasar sightline and galaxy centre) obtained from a large number of quasar sightlines passing near foreground galaxies can then be used to statistically determine the gas distribution in and around galaxies. Considerable progress has been made in mapping the distribution of gas in the CGM or galaxy halos using absorption from Lyman $-\alpha$ (Chen *et al.* 2001; Prochaska *et al.* 2011; Tumlinson *et al.* 2013; Stocke *et al.* 2013; Borthakur *et al.* 2015), Mg II (Chen *et al.* 2010; Kacprzak *et al.* 2012; Churchill *et al.* 2013; Nielsen *et al.* 2013; Bordoloi *et al.* 2014a), and other metals like C II, C III, C IV, Si II, Si III, Si IV, O VI (Tumlinson *et al.* 2011; Werk *et al.* 2014; Bordoloi *et al.* 2014b; Liang & Chen 2014). Such studies have shown that the CGM can extend upto the virial radius (∼100s of kpc); is typically cool ($\lesssim 10^5$ K, i.e. below the virial temperature); is likely to be bound to the dark matter halo of the galaxy (within $\sim\pm200\,\mathrm{km\,s^{-1}}$ of the galaxy); is multiphase in nature; and becomes progressively more ionized with increasing distance from the galaxy centre. In addition to the above, the Lyman $-\alpha$ absorbing gas is found to be ubiquitous around both star-forming and passive galaxies, while the metals are found to be more patchy in distribution.

Here we are interested in probing the high column density HI gas around galaxies. Such gas is usually traced by damped Lyman $-\alpha$ absorbers (DLAs; $N(\mathrm{HI})\geq 2\times10^{20}\,\mathrm{cm^{-2}}$) and sub-DLAs ($N(\mathrm{HI})\sim 10^{19} - 2\times10^{20}\,\mathrm{cm^{-2}}$) (see Wolfe *et al.* 2005; Péroux *et al.* 2005). Thanks to large spectroscopic surveys like the Sloan Digital Sky Survey (SDSS; York *et al.* 2000), thousands of DLAs are known at $z > 1.8$, and they are found to trace the bulk (∼80%) of the HI gas at $2 \leq z \leq 4$ (Prochaska *et al.* 2005; Noterdaeme *et al.* 2009, 2012). However, atmospheric cutoff of light below 3000 Å restricts ground-based observations of DLAs at $z < 1.5$. UV spectroscopic observations with the Hubble Space Telescope (HST) have identified ∼70 low-z ($z < 1.65$) DLAs and sub-DLAs till date (Rao *et al.* 2006, 2011; Meiring *et al.* 2011; Battisti *et al.*

2012; Turnshek *et al.* 2015; Neeleman *et al.* 2016; Rao *et al.* 2017). Using ground-based imaging studies of $z < 1$ DLAs, Rao *et al.* (2011) have found an anti-correlation (Spearman rank correlation coefficient, $r_s = -0.34$ at 3σ level of significance) between N(HI) and impact parameter (b), with median b = 17 kpc. They also do not find any correlation between galaxy luminosity and N(HI) and no significant evidence that galaxies at larger b are more luminous. Similar trend of N(HI) decreasing with b is found by Rahmani *et al.* (2016) using X-Shooter observations of $z \sim 0.6$ DLA host galaxies and by Péroux *et al.* (2012) using integral field unit observations of Hα emission from DLAs at $1 < z < 2$. At $z > 2$, Krogager *et al.* (2012) have found an anti-correlation ($r_s = -0.6$) between N(HI) and b, as well as correlation between metallicity and b, consistent with simulations that contain feedback mechanisms to control the star formation (Fynbo *et al.* 2008; Pontzen *et al.* 2008).

At $z = 0$, Zwaan *et al.* (2005b), using HI 21-cm emission maps of local galaxies, have found that N(HI) decreases with galactocentric radius. Further, they have calculated the two-dimensional probability function of HI column density and impact parameter, and found that the distribution of b and luminosities of $z < 1$ DLA host galaxies can be explained on the basis of the local galaxy population. Based on their conditional probability distribution of N(HI) and b, the expected median b for systems with log N(HI) > 20.3 (cm^{-2}) is 8 kpc. However, Rao *et al.* (2011) found that a significantly higher fraction of low-redshift DLA host galaxies are at larger b values, with luminosities less than the characteristic luminosity, which may hint at an evolution in the HI sizes of galaxies with redshift. Similar studies of HI 21-cm emission in nearby dwarf galaxies have found that their HI column density distribution function falls off significantly faster at high N(HI) compared to that in DLAs and the local luminous galaxy population (Begum *et al.* 2008; Patra *et al.* 2013). Hence, the extent of high N(HI) gas around them is likely to be much smaller and in order to detect gas with high N(HI) from dwarf galaxies one must probe them at very small impact parameters.

While Lyman $-\alpha$ absorption and HI 21-cm emission trace the neutral gas around galaxies, HI 21-cm absorption towards radio-loud quasars is an excellent tracer of the CNM phase in galaxies. A detailed study of cold HI gas in the outer disks and halos of galaxies is required to understand where and how the infalling/circumgalactic gas condenses into the ISM. There are usually two approaches to map the distribution of gas around galaxies using quasar absorption lines: (i) galaxy-blind or absorption-selected approach, where one searches for intervening absorption towards a background quasar and then tries to identify the associated host galaxy, and (ii) absorption-blind or galaxy-selected approach, where one selects a galaxy in close proximity to a background quasar (i.e. a QGP) without prior knowledge of any absorption along the quasar sightline, and then proceeds to search for absorption at the redshift of the galaxy towards the quasar. The advantage of the second approach over the first is that it is not biased against dusty sightlines (which are more likely to be conducive to the presence of cold gas), and hence it is expected to trace gas associated with the general galaxy population without any biases.

Following the second approach, HI 21-cm absorption searches from low-z ($z < 0.4$) QGPs have revealed a weak anti-correlation between the HI 21-cm optical depth and impact parameter (Carilli & van Gorkom 1992; Gupta *et al.* 2010; Borthakur *et al.* 2011; Borthakur 2016; Zwaan *et al.* 2015; Reeves *et al.* 2016). However, the number of low-z QGPs in these studies was too small to characterize the distribution of cold HI gas around galaxies. With a view to map the distribution of high column density (N(HI) $\geq 10^{19}$ cm^{-2}) cold ($T \sim$ few 100 K) HI gas around low-z galaxies, Dutta *et al.* (2017c) have carried out a systematic survey of HI 21-cm absorption in a homogeneous sample of 55 $z < 0.4$ QGPs (40 of which are in the statistical sample) towards radio sources at $b \sim$0–35 kpc. The main results from this study are highlighted below.

1. *Radial profile of cold* HI *gas around low-z galaxies:* The strength and covering factor of HI 21-cm absorption decreases, albeit slowly, with increasing impact parameter, radial distance along the galaxy's major axis and distances scaled with the effective HI radius (see Figure 2). There is a weak anti-correlation (rank correlation coefficient= -0.20 at 2.42σ level) between $\int \tau \mathrm{dv}$ and b. The covering factor of HI 21-cm absorbers decreases from $0.24^{+0.12}_{-0.08}$ at $b \leq 15$ kpc to $0.06^{+0.09}_{-0.04}$ at b = 15–35 kpc. The 3σ $\int \tau \mathrm{dv}$ sensitivity for this estimate is 0.3 km s^{-1}, which corresponds to N(HI) = 5×10^{19} cm^{-2}, for a T_s of 100 K typical of CNM and C_f of unity.
2. *Azimuthal profile of cold* HI *gas around low-z galaxies:* There is tentative evidence that the distribution of the HI 21-cm absorbers is likely to be co-planar with that of the HI disk. The absorption strength and covering factor are higher when the radio sightline passes near the galaxy's major

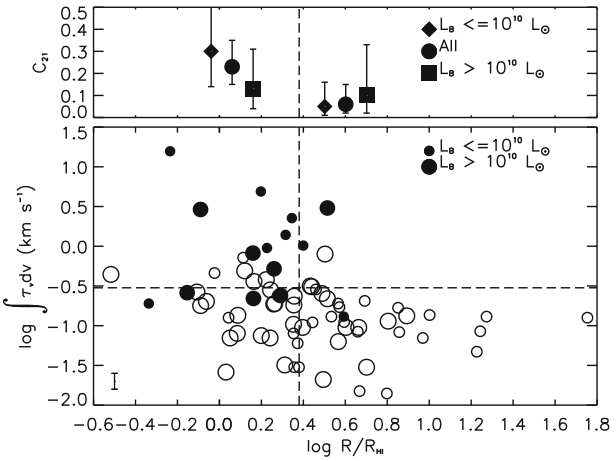

Figure 2. *Bottom*: Integrated HI 21-cm optical depth as a function of radial distance from galaxy's centre, scaled with the effective HI radius (see for details Dutta *et al.* 2017c). The solid and open circles represent measurements and 3σ upper limits (for typical velocity width of 10 km s^{-1}) of the HI 21-cm detections and non-detections, respectively. The small circles are for galaxies with luminosity, $L_B \leq 10^{10}$ $L_\odot$, while the large circles are for galaxies with $L_B > 10^{10}$ $L_\odot$. The typical error in the optical depth measurements is shown at the bottom left of the plot. The horizontal dotted line marks the optical depth sensitivity used for the covering factor estimate, i.e. $\int \tau dv = 0.3$ km s^{-1}, and the vertical dotted line marks the median scaled radial distance. *Top*: The covering factor or detection rate of HI 21-cm absorbers is shown in two different radial distance bins demarcated at the median value. The circles, diamonds and squares are for all the galaxies, galaxies with $L_B \leq 10^{10}$ $L_\odot$ and galaxies with $L_B > 10^{10}$ $L_\odot$, respectively. Both the optical depth and incidence of HI 21-cm absorption are weakly anti-correlated with distance from galaxy's centre.

axis. Further, the covering factor is maximum for sightlines that pass near the major axis of edge-on galaxies.

3 *Dependence of cold* HI *gas distribution on host galaxy properties:* The strength and covering factor of HI 21-cm absorbers is not found to depend significantly on the host galaxy properties, i.e. luminosity, stellar mass, colour, surface star formation rate density and redshift. Hence, it is surmised that the distribution of HI 21-cm absorbers is more sensitive to geometrical parameters than physical parameters related to the star formation in galaxies.

4. *Nature of cold* HI *gas around low-z galaxies:* No correlation is found between HI 21-cm optical depth and equivalent widths of Ca II and Na I absorption lines detected in the optical spectra of the quasars. The observed equivalent ratios of Ca II and Na I suggest that most of the HI 21-cm absorbers observed around low-z galaxies are not tracing the dusty star-forming disks, but rather the diffuse extended HI disks. Further, the observations suggest that cold gas clouds in the extended disks/halos of galaxies have small sizes (parsec to sub-parsec scale) and are patchy in distribution (see Figure 3). Indeed, there have been observations of structures in the HI gas around galaxies from parsec-scales (Srianand *et al.* 2013; Dutta *et al.* 2015) to kilo-parsec-scales (Dutta *et al.* 2016). This is further supported by four times higher incidence of HI 21-cm absorption around $z < 1$ DLA host galaxies (i.e. absorption-selected sample) compared to the galaxy-selected sample of QGPs. From the fact that ∼60% of $z < 1$ DLAs have cold gas that can produce detectable HI 21-cm absorption, we infer that the HI gas distribution around low-z galaxies that contribute to the DLA population is patchy, with a covering factor of ∼30% within ∼30 kpc.

5. Dependence of cold neutral gas on metals and dust

Currently it is not possible to extend the study of low-z QGPs, as described in Section 4, to higher redshifts (i.e. $z > 0.5$) due to the difficulty of constructing large spectroscopic samples of galaxies at high redshifts. Hence, the usual practice to study cold gas at high redshifts has been to search for HI 21-cm absorption towards radio-loud quasars that show strong metal or Lyman $-\alpha$ absorption in their optical and UV spectra, i.e. absorption-selected approach. As mentioned in Section 4, the Lyman $-\alpha$ line cannot observed from ground at $z < 1.5$. The Mg II doublet lines, λλ 2797, 2803, offer the best way to probe high N(HI) systems in the absence of direct observations of Lyman $-\alpha$. Mg II absorption detected towards background quasars have proved to be excellent tools to probe the gaseous halos of $z \lesssim 2$ galaxies (Lanzetta *et al.* 1987; Sargent *et al.* 1988; Bergeron & Boissé 1991; Steidel & Sargent 1992; Steidel 1995; Nestor *et al.* 2005; Prochter *et al.* 2006; Quider *et al.* 2011; Zhu & Ménard 2013). At $0.5 \leq z \leq 3.5$, systematic searches of HI 21-cm absorption in samples of Mg II systems and DLAs towards radio-loud quasars have estimated the detection rate or the CNM filling factor as 10–20% (Briggs & Wolfe 1983; Kanekar & Chengalur 2003; Curran *et al.* 2005; Gupta *et al.* 2009; Kanekar *et al.* 2009b; Curran *et al.* 2010; Srianand *et al.* 2012; Gupta *et al.* 2012; Kanekar

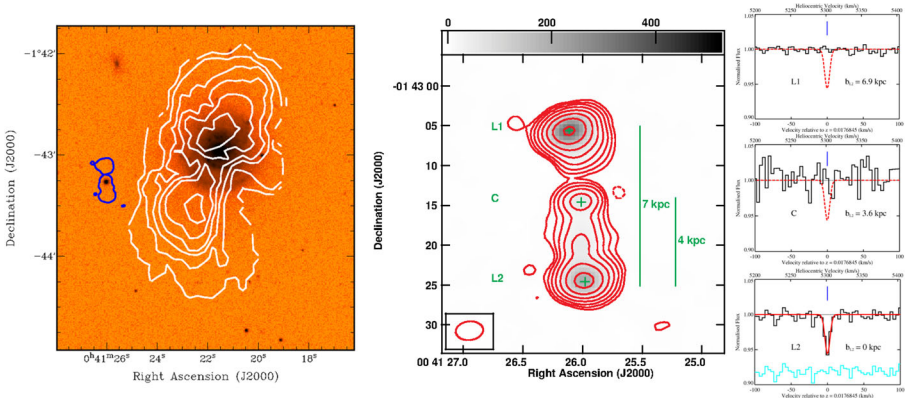

Figure 3. *Left*: SDSS r-band optical image of a QGP, overlaid with the HI emission contours of the foreground ($z = 0.02$) galaxy in white, and the outermost contour of the 1.4 GHz continuum of the background radio source in blue (see for details Dutta *et al.* 2016). *Centre*: GMRT 1.4 GHz continuum contours of the radio source that is extended over 7 kpc at the redshift of the foreground galaxy. The contour levels are plotted as $2.5 \times (-1,1,2,4,8,\ldots)$ mJy beam^{-1}, where solid (dashed) lines correspond to positive (negative) values. At the bottom left corner of the image the restoring beam is shown as an ellipse. The continuum peaks of the core, the northern lobe and the southern lobe are identified as C, L1 and L2 respectively. The vertical lines indicate the projected separation between these components at the redshift of galaxy. *Right*: GMRT HI 21-cm absorption spectra towards the different continuum components, as marked in the left panel. The best-fitting single Gaussian profile to the HI 21-cm absorption towards L2 is overplotted in solid red line, and the residuals from the fit are plotted below in cyan. This fit is also overplotted on the spectra towards L1 and C. The vertical tick marks the position of the peak optical depth detected towards L2. The HI 21-cm optical depth varies by a factor of $\geq$7 over 7 kpc at similar impact parameter of 25 kpc from the galaxy.

et al. 2013, 2014). Spin temperature (T_s) measurements derived using HI 21-cm optical depth and N(HI) measured from DLAs, suggest that most of the gas along these sightlines trace the diffuse WNM phase, and only a small fraction of the total N(HI) is associated with the CNM phase (Srianand *et al.* 2012; Kanekar *et al.* 2014). This is supported by observations of typically low ($\sim$10–20%) molecular fractions of H_2 in $z > 1.8$ DLAs (Noterdaeme *et al.* 2008), as well as physical conditions inferred in DLAs using C II* and Si II* fine structure lines (Neeleman *et al.* 2015). In addition, there are indications for an anti-correlation between T_s and the gas phase metallicity (see Kanekar *et al.* 2014, and references therein).

Strong Mg II absorbers (rest equivalent width of Mg II λ2796, $W_{\rm Mg\,II} \geq 1$ Å) at $z < 1.65$ have been shown to trace gas with high neutral hydrogen column densities, like DLAs and sub-DLAs (Rao *et al.* 2006). However, strong Mg II systems sample a wide range of galaxy impact parameters, over $\sim$10–200 kpc (Nielsen *et al.* 2013). Hence, such absorbers can trace gas in a wide variety of environments like star-forming discs, CGM, galactic winds and outflows. To study the cold dense gas around galaxies, other parameters like equivalent width ratios of metal lines are required to select sightlines that probe low impact parameters. Rao *et al.* (2006) have demonstrated that equivalent width ratios of Mg II, Mg I and Fe II absorption can be used to pre-select DLAs more successfully than by just using $W_{\rm Mg\,II}$. Further insights into the origin and physical conditions prevailing in the strong Mg II systems and DLAs can be obtained by studying their associated HI 21-cm absorption. Gupta *et al.* (2009, 2012) have shown that the HI 21-cm detection rate in strong Mg II systems can be enhanced with appropriate equivalent width ratio cuts of Mg II, Fe II and Mg I. Recently, Dutta *et al.* (2017b) have proposed an efficient Fe II absorption-based selection technique to detect high N(HI) cold gas at high-z. The detection rate of HI 21-cm absorption increases with the absorption strength of Fe II, and additional constraints on Fe II (rest equivalent width of Fe II λ2600, $W_{\rm Fe\,II} \geq 1$ Å) gives a higher (by a factor of $\sim$4) detection rate of HI 21-cm absorption compared to a pure Mg II-based selection.

Further, the properties of cold gas detected through HI 21-cm absorption are found to be closely linked with the metal and dust content of the gas. Dutta *et al.* (2017b) have found that HI 21-cm absorption arises on an average in systems with stronger metal absorption. Stacking of SDSS optical spectra of background quasars shows that the average equivalent widths of various metal lines among HI 21-cm absorbers are higher by a factor of $\sim$3–4 than that found in non-absorbers (Figure 4, left panel). In addition, quasars with HI 21-cm absorption

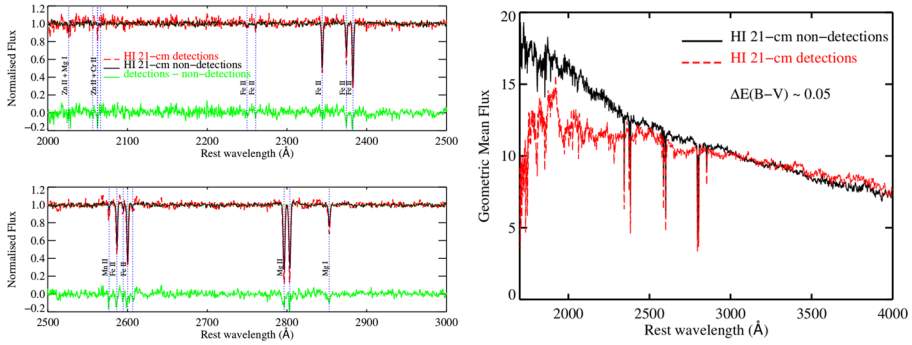

Figure 4. *Left*: The median stacked spectrum of SDSS quasars at $0.5 < z < 1.5$ which are (not) detected in HI 21-cm absorption is shown as the red dashed (black solid) line (see for details Dutta *et al.* 2017b). The difference of the stacked spectrum of HI 21-cm non-detections from that of the detections is shown as the green line at an arbitrary offset in the y-axis for clarity. The various rest wavelengths of transitions of Mg II, Mg I, Cr II, Mn II, Fe II and Zn II are marked by vertical dotted lines. The systems which show HI 21-cm absorption, also show systematically stronger metal absorption (i.e. larger equivalent widths of the metal lines by $\sim 3-4\sigma$) than those which do not. *Right*: The geometric mean stacked spectrum of SDSS quasars at $0.5 < z < 1.5$ which are (not) detected in HI 21-cm absorption is shown as the red dashed (black solid) line (see for details Dutta *et al.* 2017b). The differential reddening, $\Delta E(B-V)$, is 0.05. HI 21-cm absorption on an average causes more reddening in the quasar spectra, indicating the presence of more dust.

detected towards them are found to be systematically more reddened than those without absorption (Figure 4, right panel), and there is a tendency for the detection rate of HI 21-cm absorbers to be higher towards more reddened quasars. Further, HI 21-cm absorption searches towards radio-selected red quasars have usually resulted in a higher detection rate than that obtained for optically-selected DLAs (e.g. Carilli *et al.* 1998; Ishwara-Chandra *et al.* 2003). There have also been detections of HI 21-cm and molecular line absorption towards gravitationally-lensed systems that have high visual extinction (Carilli *et al.* 1992; Chengalur *et al.* 1999; Kanekar & Briggs 2003). Hence, all the above imply that HI 21-cm absorption is more likely to arise in metal-rich dusty cold gas.

6. Redshift evolution of cold neutral gas

The global star formation rate density (SFRD) of the Universe peaks at $z \sim 2$, followed by a decline towards $z = 0$ (Madau & Dickinson 2014). The redshift evolution of the SFRD is expected to be imprinted in the ISM/CGM of galaxies, because the physical conditions and the volume filling factors of different gas phases depend on various feedback mechanisms associated with the in-situ star-formation. Therefore, mapping the redshift evolution of different gas phases will provide deeper understanding of the physical processes that drive the global star formation in the Universe. Even more relevant for understanding the SFRD evolution is how the fraction of cold gas (which acts as the reservoir for star-formation) is evolving with redshift, which is not well-constrained from observations. The cosmic mass density of HI, $\Omega_{\rm HI}$, shows a mild (factor of ∼2–3) decrease from $2 < z < 4$ to $z \sim 0.2$ (Rhee *et al.* 2018). This is modest compared to an order of magnitude decrease in the SFRD over the same redshift range. This implies that the processes leading to the conversion of gas to stars need to be understood directly via observations of cold atomic and molecular gas. Indeed recent results using ALMA indicate that the cosmic molecular gas density peaks at $z \sim 1.5$ and drops by a factor of ~ 6.5 to $z \sim 0$ (Decarli *et al.* 2019), matching the evolution of the cosmic SFRD. Hence, the emerging picture is that cold gas content is the driving force behind the star formation history.

HI 21-cm emission and absorption measurements have been used to study in detail the CNM phase in the ISM of the Milky Way (Heiles & Troland 2003; Roy *et al.* 2013). It has been observed that ∼60% of the atomic gas is in the WNM phase and ∼50% of the WNM lies in the thermally unstable range of 500–5000 K. Jenkins & Tripp (2001) also arrived at similar conclusions based on excitation of neutral carbon using UV spectroscopy. The ideal, i.e. dust- and luminosity-unbiased, way to estimate the redshift evolution of the cold gas fraction would be to conduct blind HI 21-cm absorption searches. However, this has not been possible till recently due to limited receiver bandwidths and hostile radio frequency interference environment, though the situation is now improving with the advent of Square Kilometer Array (SKA) pre-cursors and induction of wide-band receivers in

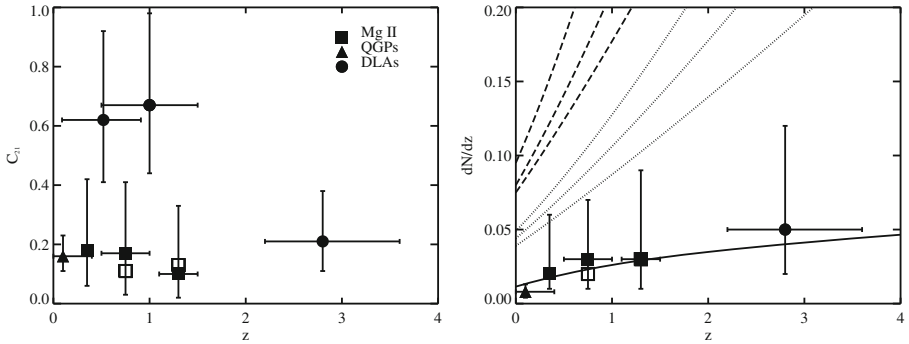

Figure 5. Redshift evolution of detection rate (left) and number density per unit redshift (right) of HI 21-cm absorbers. The triangles, squares and circles represent estimates based on QGPs, strong Mg II systems and DLAs, respectively, from literature compilations (Lane 2000; Gupta *et al.* 2009, 2012; Srianand *et al.* 2012; Kanekar *et al.* 2009b, 2014; Dutta *et al.* 2017c, b, a). The open symbols represent estimates that have been corrected for partial coverage whenever possible (see for details Gupta *et al.* 2012). The dashed and dotted lines in the right panel shows for reference the redshift evolution of the number of strong Mg II absorbers ($W_{\rm Mg\,II} \geq 1$ Å) per unit redshift (Prochter *et al.* 2006), and the number of DLAs per unit redshift (Rao *et al.* 2006), respectively. The solid line is the curve for non-evolving population of HI 21-cm absorbers normalized at $z = 1.3$. The next challenge for HI 21-cm absorption line studies would be to reduce the large uncertainties, statistical and systematic, on these measurements, through blind unbiased searches for absorbers.

existing telescopes. Till date, HI 21-cm absorption studies have been typically conducted in samples of QGPs (see Section 4) or absorption-selected samples (see Section 5). Figure 5 summarizes the detection rates of HI 21-cm absorption and the number density per unit redshift of HI 21-cm absorbers (n_{21}) obtained using different techniques at different redshifts. No significant evolution is observed in the detection rate and n_{21} among strong Mg II systems over $0.3 < z < 1.5$. However, comparing HI 21-cm studies of $z > 2$ and $z < 1$ DLAs, it can be seen that the cold gas fraction in DLAs may be declining with redshift, with the detection rate being $\sim$3 times lower at $z > 2$ compared to $z < 1$.

Besides the evolution in incidence, Kanekar *et al.* (2014) have found evidence for redshift evolution in DLA spin temperatures. The $T_{\rm s}$ distribution of $z > 2$ DLAs is found to be significantly different from that of $z < 2$ DLAs, and the high temperatures in high-z DLAs are attributed to lower fractions of CNM. Further, Dutta *et al.* (2017b) have found an increasing trend of the velocity width of the HI 21-cm absorption lines with redshift. A possible explanation for this is that the typical HI 21-cm absorber may be probed by larger mass galaxy halos at high-z (for a given metallicity). In addition, taking into account the evolution of size and luminosity of galaxies with redshift, the radius of the cold HI gas around a galaxy that gives rise to HI 21-cm absorption is likely be much higher at high-z than what is seen at low-z for a galaxy with same optical luminosity.

While we have made progress in understanding the nature of cold HI gas in galaxies and its redshift evolution, it can be seen that we are still limited by statistical uncertainties due to the small number of detections and different sample selection techniques at different redshifts. Hence, increasing the number of HI 21-cm detections over $0 < z < 2$, such that we can uniformly trace the evolution of cold gas in galaxies in a dust- and luminosity-unbiased way, is one of the major motivations of the upcoming blind HI 21-cm absorption line surveys using the SKA pathfinders and pre-cursors, e.g. FLASH/ASKAP, MALS/MeerKAT, SHARP/Apertif (Gupta *et al.* 2016; Maccagni *et al.* 2017).

7. Summary and future perspectives

We have discussed in this work the results from different efforts to study the cold neutral gas in and around galaxies using HI 21-cm absorption. Some of the key results from these studies are summarized here.

- The cold neutral gas around $z < 0.4$ galaxies, as traced by HI 21-cm absorption, has a weakly declining radial profile, with an average covering factor of $0.16^{+0.07}_{-0.05}$ within 30 kpc. Based on geometrical and chemical analysis, the HI 21-cm absorbers are likely tracing the diffuse extended HI disc around galaxies. The cold HI gas is patchily distributed around galaxies and can have variations in the optical depth at both parsec- and kilo-parsec-scales.

- The detection rate and optical depth of HI 21-cm absorption over $0.5 < z < 1.5$ are correlated with the equivalent width of metal line absorption like Mg II and Fe II. They are further correlated with the reddening of the background quasar. Thus, the presence and amount of cold HI gas in the vicinity of high-z galaxies appear to be closely related to the metal and dust content of the gas.
- The incidence and number density per unit redshift of HI 21-cm absorbers in strong Mg II absorbers do not seem to evolve over $0.3 < z < 1.5$, albeit the uncertainties are still large. The incidence of HI 21-cm absorbers in DLAs, on the other hand, seem to show a stronger evolution, i.e. it increases by a factor of $\sim$3 from $z > 2$ to $z < 1$. The spin temperature of DLAs also show a redshift evolution, with $z > 2$ DLAs having significantly higher T_s.

HI 21-cm absorption towards background radio-loud quasars has thus proved to be an effective tool to map the distribution of cold neutral gas around foreground low-z galaxies, as well as study the neutral gas in the vicinity of high-z galaxies selected via Mg II absorption or DLAs. The next step is to increase the number of sightlines searched for HI 21-cm absorption and the number of detections through blind surveys as mentioned in Section 6. The large number (few hundreds) of HI 21-cm absorption detection is expected to accurately characterize the redshift evolution of cold gas in galaxies. Here we identify few prospects involving multi-wavelength observations that are promising for interpreting the existing and upcoming results with HI 21-cm absorption.

1. High resolution ($R \sim 40000$) optical spectroscopy of quasars which show HI 21-cm absorption will enable detailed comparison of the kinematics of metals and HI gas, and confirm with higher significance the various trends of HI with metals and dust as found using low resolution optical spectra (e.g. Srianand *et al.* 2012).
2. Sub-arcsecond-scale imaging of the background radio sources will allow us to quantify the covering factor of cold gas and study its small scale structure (e.g. Gupta *et al.* 2012).
3. OH and CO absorption spectroscopy of HI 21-cm absorbers will facilitate comparison of the kinematics and structure of neutral and molecular gas phases in and around galaxies (e.g. Gupta *et al.* 2018a; Combes *et al.* 2019).
4. Identifying the host galaxies of high-z HI 21-cm absorbers using optical integral field unit spectroscopy (e.g. MUSE/VLT) and molecular emission with e.g. ALMA, is essential to connect the properties of the galaxies with the absorbing gas (e.g. Péroux *et al.* 2019). Such observations are also required to link the neutral gas around galaxies with their ionized and molecular gas content, and hence understand the mechanisms through which galaxies acquire the fuel for forming stars.

The upcoming surveys will provide interesting targets for follow-up multi-wavelength observations as outlined above. In addition, existing and planned wide-area multi-object/integral field optical spectroscopic surveys like Calar Alto Legacy Integral Field Area (CALIFA; Sánchez *et al.* 2012), Sydney-Australian-Astronomical-Observatory Multiobject Integral-Field Spectrograph (SAMI; Croom *et al.* 2012), SDSS Mapping Nearby Galaxies at Apache Point Observatory (MaNGA; Bundy *et al.* 2015) and WEAVE (Dalton *et al.* 2012), will complement the HI 21-cm surveys in associating the absorption with the galaxies.

Acknowledgements

I thank the anonymous reviewers for their helpful comments. I thank Raghunathan Srianand for going through a draft of this review and providing feedback. I am grateful to the Alexander von Humboldt Foundation for support in the form of a post-doctoral fellowship.

References

Bagetakos, I., Brinks, E., Walter, F., *et al.* 2011, AJ, 141, 23
Bahcall, J. N., Ekers, R. D. 1969, ApJ, 157, 1055
Battisti, A. J., Meiring, J. D., Tripp, T. M., *et al.* 2012, ApJ, 744, 93
Begeman, K. G. 1987, PhD thesis, Kapteyn Institute
Begum, A., Chengalur, J. N., Karachentsev, I. D., Sharina, M. E., Kaisin, S. S. 2008, MNRAS, 386, 1667
Bergeron, J., Boissé, P. 1991, A&A, 243, 344
Biggs, A. D., Zwaan, M. A., Hatziminaoglou, E., Péroux, C., Liske, J. 2016, MNRAS, 462, 2819
Bordoloi, R., Lilly, S. J., Kacprzak, G. G., Churchill, C. W. 2014a, ApJ, 784, 108
Bordoloi, R., Tumlinson, J., Werk, J. K., *et al.* 2014b, ApJ, 796, 136
Borthakur, S. 2016, ApJ, 829, 128

Borthakur, S., Tripp, T. M., Yun, M. S., *et al.* 2011, ApJ, 727, 52
Borthakur, S., Heckman, T., Tumlinson, J., *et al.* 2015, ApJ, 813, 46
Bosma, A. 1978, PhD thesis, PhD Thesis, Groningen Univ.
Bosma, A. 1981a, AJ, 86, 1791
Bosma, A. 1981b, AJ, 86, 1825
Braun, R. 1997, ApJ, 484, 637
Briggs, F. H., Wolfe, A. M. 1983, ApJ, 268, 76
Broeils, A. H. 1992, A&A, 256, 19
Brown, R. L., Roberts, M. S. 1973, ApJ, 184, L7
Bundy, K., Bershady, M. A., Law, D. R., *et al.* 2015, ApJ, 798, 7
Carilli, C. L., Menten, K. M., Reid, M. J., Rupen, M. P., Yun, M. S. 1998, ApJ, 494, 175
Carilli, C. L., Perlman, E. S., Stocke, J. T. 1992, ApJ, 400, L13
Carilli, C. L., van Gorkom, J. H. 1992, ApJ, 399, 373
Carilli, C. L., Menten, K. M., Stocke, J. T., *et al.* 2000, Phys. Rev. Lett., 85, 5511
Catinella, B., Cortese, L. 2015, MNRAS, 446, 3526
Chang, T.-C., Pen, U.-L., Bandura, K., Peterson, J. B. 2010, Nature, 466, 463
Chen, H.-W., Helsby, J. E., Gauthier, J.-R., *et al.* 2010, ApJ, 714, 1521
Chen, H.-W., Lanzetta, K. M., Webb, J. K., Barcons, X. 2001, ApJ, 559, 654
Chengalur, J. N., de Bruyn, A. G., Narasimha, D. 1999, A&A, 343, L79
Chengalur, J. N., Kanekar, N. 2003, Phys. Rev. Lett., 91, 241302
Chung, A., van Gorkom, J. H., Kenney, J. D. P., Crowl, H., Vollmer, B. 2009, AJ, 138, 1741
Churchill, C. W., Nielsen, N. M., Kacprzak, G. G., Trujillo-Gomez, S. 2013, ApJ, 763, L42
Clark, B. G., Radhakrishnan, V., Wilson, R. W. 1962, ApJ, 135, 151
Combes, F., Gupta, N., Jozsa, G. I. G., Momjian, E. 2019, A&A, 623, A133
Croom, S. M., Lawrence, J. S., Bland-Hawthorn, J., *et al.* 2012, MNRAS, 421, 872
Curran, S. J., Murphy, M. T., Pihlström, Y. M., Webb, J. K., Purcell, C. R. 2005, MNRAS, 356, 1509
Curran, S. J., Tzanavaris, P., Darling, J. K., *et al.* 2010, MNRAS, 402, 35
Dalton, G., Trager, S. C., Abrams, D. C., *et al.* 2012, in Proc. SPIE, Vol. 8446, Ground-based and Airborne Instrumentation for Astronomy IV, 84460P
de Blok, W. J. G., Walter, F., Brinks, E., *et al.* 2008, AJ, 136, 2648
Decarli, R., Walter, F., Gonzalez-Lopez, J., *et al*. 2019, ApJ, 882, 138
Delhaize, J., Meyer, M. J., Staveley-Smith, L., Boyle, B. J. 2013, MNRAS, 433, 1398
Dickey, J. M., Kulkarni, S. R., van Gorkom, J. H., Heiles, C. E. 1983, ApJS, 53, 591
Dickey, J. M., Mebold, U., Stanimirovic, S., Staveley-Smith, L. 2000, ApJ, 536, 756
Dutta, R., Gupta, N., Srianand, R., O'Meara, J. M. 2016, MNRAS, 456, 4209
Dutta, R., Srianand, R., Gupta, N., Joshi, R. 2017a, MNRAS, 468, 1029
Dutta, R., Srianand, R., Gupta, N., *et al.* 2017b, MNRAS, 465, 4249
Dutta, R., Srianand, R., Gupta, N., *et al.* 2017c, MNRAS, 465, 588
Dutta, R., Srianand, R., Muzahid, S., *et al.* 2015, MNRAS, 448, 3718
Ewen, H. I., Purcell, E. M. 1951, Nature, 168, 356
Fernández, X., Gim, H. B., van Gorkom, J. H., *et al.* 2016, ApJ, 824, L1
Field, G. B. 1959, ApJ, 129, 536
Field, G. B., Goldsmith, D. W., Habing, H. J. 1969, ApJ, 155, L149
Fynbo, J. P. U., Prochaska, J. X., Sommer-Larsen, J., Dessauges-Zavadsky, M., Møller, P. 2008, ApJ, 683, 321
Gupta, N., Momjian, E., Srianand, R., *et al.* 2018a, ApJ, 860, L22
Gupta, N., Srianand, R., Bowen, D. V., York, D. G., Wadadekar, Y. 2010, MNRAS, 408, 849
Gupta, N., Srianand, R., Petitjean, P., *et al.* 2012, A&A, 544, A21
Gupta, N., Srianand, R., Petitjean, P., Noterdaeme, P., Saikia, D. J. 2009, MNRAS, 398, 201
Gupta, N., Srianand, R., Baan, W., *et al.* 2016, in Proceedings of MeerKAT Science: On the Pathway to the SKA. 25-27 May, 2016 Stellenbosch, South Africa (MeerKAT2016), 14
Gupta, N., Srianand, R., Farnes, J. S., *et al.* 2018b, MNRAS, 476, 2432
Hagen, J. P., Lilley, A. E., McClain, E. F. 1955, ApJ, 122, 361
Hagen, J. P., McClain, E. F. 1954, ApJ, 120, 368
Hagen, J. P., McClain, E. F., Hepburn, N. 1954, AJ, 59, 323
Haynes, M. P., Giovanelli, R., Roberts, M. S. 1979, ApJ, 229, 83
Heiles, C., Miley, G. K. 1970, ApJ, 160, L83
Heiles, C., Troland, T. H. 2003, ApJ, 586, 1067
Heiles, C., Troland, T. H. 2004, ApJS, 151, 271
Hopkins, A. M., Beacom, J. F. 2006, ApJ, 651, 142
Hoppmann, L., Staveley-Smith, L., Freudling, W., *et al.* 2015, MNRAS, 452, 3726
Ianjamasimanana, R., de Blok, W. J. G., Walter, F., Heald, G. H. 2012, AJ, 144, 96
Ishwara-Chandra, C. H., Dwarakanath, K. S., Anantharamaiah, K. R. 2003, J. Astrophys. Astron., 24, 37
Jenkins, E. B., Tripp, T. M. 2001, ApJS, 137, 297
Jones, M. G., Haynes, M. P., Giovanelli, R., Moorman, C. 2018, MNRAS, 477, 2
Kacprzak, G. G., Churchill, C. W., Nielsen, N. M. 2012, ApJ, 760, L7

Kanekar, N., Briggs, F. H. 2003, A&A, 412, L29
Kanekar, N., Chengalur, J. N. 2003, AA, 399, 857
Kanekar, N., Chengalur, J. N., Ghosh, T. 2010, ApJ, 716, L23
Kanekar, N., Chengalur, J. N., Subrahmanyan, R., Petitjean, P. 2001, A&A, 367, 46
Kanekar, N., Ellison, S. L., Momjian, E., York, B. A., Pettini, M. 2013, MNRAS, 428, 532
Kanekar, N., Lane, W. M., Momjian, E., Briggs, F. H., Chengalur, J. N. 2009a, MNRAS, 394, L61
Kanekar, N., Langston, G. I., Stocke, J. T., Carilli, C. L., Menten, K. M. 2012, ApJ, 746, L16
Kanekar, N., Prochaska, J. X., Ellison, S. L., Chengalur, J. N. 2009b, MNRAS, 396, 385
Kanekar, N., Sethi, S., Dwarakanath, K. S. 2016, ApJ, 818, L28
Kanekar, N., Prochaska, J. X., Smette, A., *et al.* 2014, MNRAS, 438, 2131
Keeney, B. A., Stocke, J. T., Danforth, C. W., Carilli, C. L. 2011, AJ, 141, 66
Krogager, J.-K., Fynbo, J. P. U., Møller, P., *et al.* 2012, MNRAS, 424, L1
Kulkarni, S. R., Heiles, C. 1987, in Astrophysics and Space Science Library, Vol. 134, Interstellar Processes, ed. D. J. Hollenbach & H. A. Thronson, Jr., 87–122
Kulkarni, S. R., Heiles, C. 1988, Neutral hydrogen and the diffuse interstellar medium, ed. K. I. Kellermann G. L. Verschuur, 95–153
Lah, P., Chengalur, J. N., Briggs, F. H., *et al.* 2007, MNRAS, 376, 1357
Lah, P., Pracy, M. B., Chengalur, J. N., *et al.* 2009, MNRAS, 399, 1447
Lane, W. M. 2000, PhD thesis, University of Groningen
Lanzetta, K. M., Turnshek, D. A., Wolfe, A. M. 1987, ApJ, 322, 739
Liang, C. J., Chen, H.-W. 2014, MNRAS, 445, 2061
Liszt, H. 2001, A&A, 371, 698
Maccagni, F. M., Morganti, R., Oosterloo, T. A., Geréb, K., Maddox, N. 2017, A&A, 604, A43
Madau, P., Dickinson, M. 2014, ARA&A, 52, 415
Masui, K. W., Switzer, E. R., Banavar, N., *et al.* 2013, ApJ, 763, L20
McKee, C. F., Ostriker, J. P. 1977, ApJ, 218, 148
Mebold, U., Düsterberg, C., Dickey, J. M., Staveley-Smith, L., Kalberla, P. 1997, ApJ, 490, L65
Meiring, J. D., Tripp, T. M., Prochaska, J. X., *et al.* 2011, ApJ, 732, 35
Mihos, J. C., Keating, K. M., Holley-Bockelmann, K., Pisano, D. J., Kassim, N. E. 2012, ApJ, 761, 186
Morganti, R., Oosterloo, T. 2018, A&A Rev., 26, 4
Muller, C. A., Oort, J. H. 1951, Nature, 168, 357
Neeleman, M., Prochaska, J. X., Ribaudo, J., *et al.* 2016, ApJ, 818, 113
Neeleman, M., Prochaska, J. X., Wolfe, A. M. 2015, ApJ, 800, 7
Nestor, D. B., Turnshek, D. A., Rao, S. M. 2005, ApJ, 628, 637
Nielsen, N. M., Churchill, C. W., Kacprzak, G. G., Murphy, M. T. 2013, ApJ, 776, 114
Noterdaeme, P., Ledoux, C., Petitjean, P., Srianand, R. 2008, A&A, 481, 327
Noterdaeme, P., Petitjean, P., Ledoux, C., Srianand, R. 2009, A&A, 505, 1087
Noterdaeme, P., Petitjean, P., Carithers, W. C., *et al.* 2012, A&A, 547, L1
Oosterloo, T., Fraternali, F., Sancisi, R. 2007, AJ, 134, 1019
Patra, N. N., Chengalur, J. N., Begum, A. 2013, MNRAS, 429, 1596
Pawsey, J. L. 1951, Nature, 168, 358
Péroux, C., Bouché, N., Kulkarni, V. P., York, D. G., Vladilo, G. 2012, MNRAS, 419, 3060
Péroux, C., Dessauges-Zavadsky, M., D'Odorico, S., Sun Kim, T., McMahon, R. G. 2005, MNRAS, 363, 479
Péroux, C., Zwaan, M. A., Klitsch, A., *et al.* 2019, MNRAS, 485, 1595
Pontzen, A., Governato, F., Pettini, M., *et al.* 2008, MNRAS, 390, 1349
Prochaska, J. X., Herbert-Fort, S., Wolfe, A. M. 2005, ApJ, 635, 123
Prochaska, J. X., Weiner, B., Chen, H.-W., Mulchaey, J., Cooksey, K. 2011, ApJ, 740, 91
Prochter, G. E., Prochaska, J. X., Burles, S. M. 2006, ApJ, 639, 766
Quider, A. M., Nestor, D. B., Turnshek, D. A., *et al.* 2011, AJ, 141, 137
Rahmani, H., Srianand, R., Gupta, N., *et al.* 2012, MNRAS, 425, 556
Rahmani, H., Péroux, C., Turnshek, D. A., *et al.* 2016, MNRAS, 463, 980
Rao, S. M., Belfort-Mihalyi, M., Turnshek, D. A., *et al.* 2011, MNRAS, 416, 1215
Rao, S. M., Turnshek, D. A., Nestor, D. B. 2006, ApJ, 636, 610
Rao, S. M., Turnshek, D. A., Sardane, G. M., Monier, E. M. 2017, MNRAS, 471, 3428
Reeves, S. N., Sadler, E. M., Allison, J. R., *et al.* 2016, MNRAS, 457, 2613
Rhee, J., Lah, P., Briggs, F. H., *et al.* 2018, MNRAS, 473, 1879
Rhee, J., Zwaan, M. A., Briggs, F. H., *et al.* 2013, MNRAS, 435, 2693
Roberts, M. S. 1970, ApJ, 161, L9
Rohlfs, K., Wilson, T. L. 2000, Tools of radio astronomy
Rosenberg, J. L., Schneider, S. E. 2002, ApJ, 567, 247
Roy, N., Chengalur, J. N., Srianand, R. 2006, MNRAS, 365, L1
Roy, N., Kanekar, N., Chengalur, J. N. 2013, MNRAS, 436, 2366
Rubin, V. C., Burstein, D., Ford, Jr., W. K., Thonnard, N. 1985, ApJ, 289, 81

Sánchez, S. F., Kennicutt, R. C., Gil de Paz, A., *et al.* 2012, A&A, 538, A8
Sancisi, R., Fraternali, F., Oosterloo, T., van der Hulst, T. 2008, A&A Rev., 15, 189
Sargent, W. L. W., Steidel, C. C., Boksenberg, A. 1988, ApJ, 334, 22
Shuter, W. L. H., Gower, J. F. R. 1969, Nature, 223, 1046
Srianand, R., Gupta, N., Petitjean, P., *et al.* 2012, MNRAS, 421, 651
Srianand, R., Gupta, N., Rahmani, H., *et al.* 2013, MNRAS, 428, 2198
Steidel, C. C. 1995, in QSO Absorption Lines, ed. G. Meylan, 139
Steidel, C. C., Sargent, W. L. W. 1992, ApJS, 80, 1
Stocke, J. T., Keeney, B. A., Danforth, C. W., *et al.* 2013, ApJ, 763, 148
Tamburro, D., Rix, H.-W., Leroy, A. K., *et al.* 2009, AJ, 137, 4424
Tumlinson, J., Peeples, M. S., Werk, J. K. 2017, ARA&A, 55, 389
Tumlinson, J., Thom, C., Werk, J. K., *et al.* 2011, Science, 334, 948
Tumlinson, J., Thom, C., Werk, J. K., *et al.* 2013, ApJ, 777, 59
Turnshek, D. A., Monier, E. M., Rao, S. M., *et al.* 2015, MNRAS, 449, 1536
van Albada, T. S., Bahcall, J. N., Begeman, K., Sancisi, R. 1985, ApJ, 295, 305
van de Hulst, H. C. 1945, Nederl. Tij. Natuurkunde, 11, 201
van der Hulst, J. M., van Albada, T. S., Sancisi, R. 2001, in Astronomical Society of the Pacific Conference Series, Vol. 240, Gas and Galaxy Evolution, ed. J. E. Hibbard, M. Rupen, J. H. van Gorkom, 451
Verheijen, M., van Gorkom, J. H., Szomoru, A., *et al.* 2007, ApJ, 668, L9
Wakker, B. P., Lockman, F. J., Brown, J. M. 2011, ApJ, 728, 159
Walter, F., Brinks, E., de Blok, W. J. G., *et al.* 2008, AJ, 136, 2563
Werk, J. K., Prochaska, J. X., Tumlinson, J., *et al.* 2014, ApJ, 792, 8
Wolfe, A. M., Briggs, F. H., Jauncey, D. L. 1981, ApJ, 248, 460
Wolfe, A. M., Briggs, F. H., Turnshek, D. A., *et al.* 1985, ApJ, 294, L67
Wolfe, A. M., Brown, R. L., Roberts, M. S. 1976, Phys. Rev. Lett., 37, 179
Wolfe, A. M., Davis, M. M. 1979, AJ, 84, 699
Wolfe, A. M., Gawiser, E., Prochaska, J. X. 2005, ARA&A, 43, 861
Wolfire, M. G., Hollenbach, D., McKee, C. F., Tielens, A. G. G. M., Bakes, E. L. O. 1995, ApJ, 443, 152
Wolfire, M. G., McKee, C. F., Hollenbach, D., Tielens, A. G. G. M. 2003, ApJ, 587, 278
York, D. G., Adelman, J., Anderson, Jr., J. E., *et al.* 2000, AJ, 120, 1579
Zhu, G., Ménard, B. 2013, ApJ, 770, 130
Zwaan, M. A., Liske, J., Péroux, C., *et al.* 2015, MNRAS, 453, 1268
Zwaan, M. A., Meyer, M. J., Staveley-Smith, L., Webster, R. L. 2005a, MNRAS, 359, L30
Zwaan, M. A., van der Hulst, J. M., Briggs, F. H., Verheijen, M. A. W., Ryan-Weber, E. V. 2005b, MNRAS, 364, 1467
Zwaan, M. A., van Dokkum, P. G., Verheijen, M. A. W. 2001, Science, 293, 1800